Journal of Applied Biomechanics, 2010, 26, 10-16
© 2010 Human Kinetics, Inc.

Stiffness and Endurance of a Locking Compression Plate Fixed on Fractured Femur

Chaosuan Kanchanomai, Panurungsit Muanjan, and Vajara Phiphobmongkol

The effects of locking screw position (long column fixation—long distance between the nearest screws to the fracture—and short column fixation—short distance between the nearest screws to the fracture) and fracture gap size (1-mm and 8-mm transverse fracture gap) on stiffness and fatigue of fractured femur fixed with a locking compression plate (LCP) were biomechanically evaluated. The stiffness of 1-mm fracture gap models and that of intact femoral model were in the range of 270–284 N/mm, while those of 8-mm fracture gap models were significantly lower (155–170 N/mm). After 1,000,000 cycles of loading, no fracture of LCP of 1-mm fracture gap models fixed in either long column or short column fashions occurred. On the other hand, the complete fractures of LCPs of 8-mm fracture gap models fixed in long column and short column fashions occurred after 51,500 and 42,000 cycles of loading, respectively. These results suggest that the full weight loading may be allowed for the patient with 1-mm transverse femoral fracture fixed with an LCP. On the other hand, the full load of walking should be avoided for the patient with 8-mm transverse femoral fracture fixed with an LCP before adequate healing.

Keywords: locking compression plate, femur, fatigue, stiffness

The dynamic compression plate (DCP) is one of the most commonly implants used for internal fixation. To obtain a stable fixation, the screws on the DCP must be pressed or tightened into the DCP holes; therefore, a high amount of compression load is transmitted from the screws through the bone-plate interface. Thus, the stability of bone and plate system is achieved (Thakur, 1997). However, the existing compression force between bone and plate may cause the cortical vascular damage, create localized osteopenia, and compromise bone healing. To reduce these disadvantages, the locking compression plate (LCP) has combined the advantages of compression hole in DCP with the advantages of threaded hole, that is, a combination hole (Aslam et al., 2005; Frigg, 2003). The threaded part of the combination hole is designed to use with a locking head screw. If the locking head screws are fastened through the conical thread holes of LCP, the load is transmitted through the screw-plate system without compression between plate and bony cortex. This is done not only to preserve the bony vascular supply, but also to provide angular stability to the fracture. The accurate contouring of plate can be avoided because there is no direct contact between plate and bony cortex. Moreover, an ordinary cortical screw can be used through the conventional compression hole to function as ordinary DCP. The LCP system is therefore possible to serve both purposes, that of the compression plate system or locking plate system. As the treatment of fracture using LCP is increasing, more clinical studies have been reported and the advantages of this system have been confirmed (Leung et al., 2003; Sommer et al., 2003). Treatment of femoral-shaft fracture with LCP is thus an alternative, and has become more popular in treating some indicated cases.

In addition to the stability and biological compatibility of plate to treat the femoral fracture, the durability of plate is one of the crucial considerations. If partial load of walking is allowed before complete healing, the fatigue damage of plate (a process of defect accumulation, crack initiation, and crack propagation with number of load cycles) is possible even under a low magnitude of cyclic load (Azevedo, 2003; Sivakumar et al., 1994; Stoffel et al., 2003; Sudhakar, 2005; Van Meeteren et al., 1996). The question that commonly arises during screw fixation is how to place the screws on each main fragment—that is, long column fixation (long distance between the screws nearest the fracture) or short column fixation (short distance between the screws nearest the fracture)—to obtain the appropriate stability and endurance. Unfortunately, few reports regarding stability and endurance of the long bone fracture fixed with an internal fixator are available. Therefore, the purpose of this work was to biomechanically evaluate the effects of locking screw position (long column and short column fixations) and fracture gap size

Kanchanomai and Muanjan are with the Department of Mechanical Engineering, Faculty of Engineering, Thammasat University, Klong-Luang, Pathumthani, Thailand. Phiphobmongkol is with the Department of Orthopedic Surgery, Bhumibol Adulyadej Hospital, Royal Thai Air Force, Bangkok, Thailand.

(1-mm and 8-mm interfragmentary gaps) on stiffness and endurance of an LCP fixed on diaphyseal-fractured composite-femur. The clinical relevance of results was also discussed.

Methods

Stiffness and Strain Distribution Tests

To avoid the interspecimen variations of the human femurs in different cadavers, the composite large left femurs (Third-generation femur—3306, Pacific Research Laboratories, Inc., USA) were used for this study. Its mechanical properties are listed in Table 1. With geometry and mechanical properties similar to those of young human femurs, this composite femur has been successfully used in many biomechanical research studies (Cristofolini et al., 1996; Heiner & Brown, 2001; Waide et al., 2003). Fourteen holes broad LCP (Synthes—226.641 with 250 mm-length) and four locking head screws (Synthes—213.344 with 4 mm-diameter and 45 mm-length) were fixed on the composite femur. The LCP and locking head screw are made from 316L stainless steel. The mechanical properties of 316L stainless steel are given in Table 1. The effects of position of locking head screw and fracture gap size on stiffness and strain distribution of the composite femur fixed with LCP were studied using five femoral models (Figure 1), as follows.

Model 1: an intact composite femur

Model 2: a transverse fracture (1-mm gap) on the midshaft of femur fixed with an LCP using long column fixation method (four locking screws fixed in hole numbers 1, 3 and 12, 14)

Model 3: similar fractured pattern as model 2; however, an LCP was fixed using short column fixation methods (four locking screws fixed in hole numbers 1, 6 and 9, 14)

Model 4: a transverse fracture (8-mm gap) on the midshaft of femur fixed with an LCP using long column fixation method (four locking screws fixed in hole numbers 1, 3 and 12, 14)

Model 5: similar fractured pattern as model 4; however, an LCP was fixed using short column fixation methods (four locking screws fixed in hole numbers 1, 6 and 9, 14)

Transverse fractures of the femoral models were created using a saw blade, which resulted in 1-mm transverse fracture gap for models 2 and 3, and 8-mm transverse fracture gap for models 4 and 5. The 1-mm transverse fracture gap was used to represent a simple and stable fracture (no gap or very small gap), whereas the 8-mm transverse fracture gap was used to represent the comminuted fracture. The fixation of the locking screws and the LCPs on the composite femurs was performed in accordance with the standard procedure used in fixation of human femur, as well as those recommended in large fragment LCP technical guide provided from the producer (Synthes, Inc.).

A monotonic loading model is shown in Figure 2. This model took into account the forces acting through the ilio-tibial tract in the frontal plane, as well as those forces acting on the femoral condyles in the sagittal plane (Cordey et al., 1999). During tests, this loading model produced compression on both femoral head and femoral condyles in vertical direction, and simulated the tension force acting at the greater trochanter. The distal femur was supported by a pin and ball bearing to prevent undesirable moment and torque. Loadings were performed using a servo-hydraulic fatigue machine (Instron 8872 with 5-kN load cell) under 25°C and 55% relative humidity.

Based on the body weight of a young Thai male (60 kg), the femoral models were compressed from 0 N to 600 N under a 60 N/s loading rate. The models were held without loading for more than 30 min before the next loading to relax the time-dependent deformation of composite femur. The strain gages with 0.3-mm gauge length (Texas Measurements, Inc., FLA-03-11) were set on the surface of LCP, as schematically shown in Figure 1. During the test, loads as well as deformations of the models were recorded by the controller of a servo-hydraulic fatigue machine, while the strains on the surface of LCP were collected using computerized data acquisition system (National Instrument: PCI-6013 and LabVIEW 7.0). After unloading, the screw torque was checked for screw loosening, and the strains of LCPs and deformations of models were checked for plastic deformation.

The stiffness of femoral model was defined as the ratio between compression load and the deformation of the model. Because there was no significant interspecimen variation of the composite femur (Cristofolini et al., 1996; Heiner & Brown, 2001; Waide et al., 2003) and the deformation of the present LCP was expected

Table 1 Mechanical properties of composite femur and LCP

		Tensile		Compressive	
Material	**Density (g/cc)**	**Modulus (MPa)**	**Strength (MPa)**	**Modulus (MPa)**	**Strength (MPa)**
Cortical bone	1.7	12,400	90	7,600	120
Cancellous bone	0.27	—	—	104	4.8
316L stainless steel	8	193×10^3	595	—	—

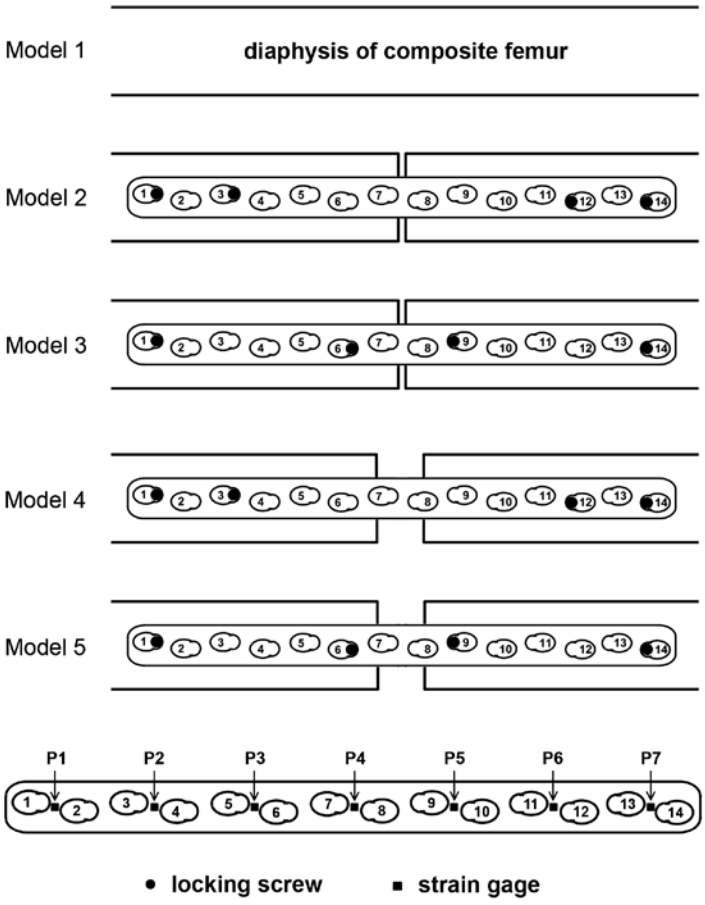

Figure 1 — Schematic representation of LCP-composite femoral models. Model **1**, an intact femur; model **2**, a fractured femur (1-mm gap) fixed with an LCP using the long column fixation method; model **3**, a fractured femur (1-mm gap) fixed with an LCP using the short column fixation method; model **4**, a fractured femur (8-mm gap) fixed with an LCP using the long column fixation method; and model **5,** a fractured femur (8-mm gap) fixed with an LCP using the short column fixation method.

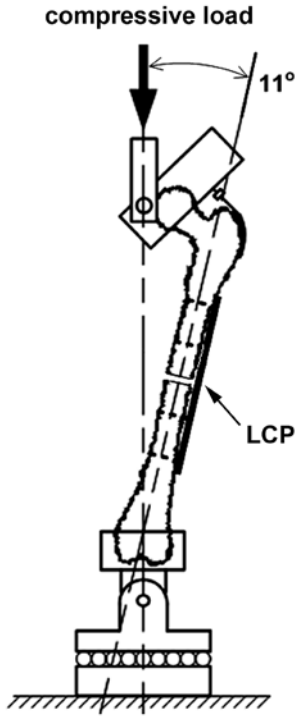

Figure 2 — Experimental system for monotonic loading of composite femur.

to be elastic, a specimen was then used in each model. However, the loadings were performed five times in every test conditions ($n = 5$), and the means and standard deviations (SDs) of stiffness and strains were calculated. The confidence intervals (CIs) with significant level (α) of 0.05 were also determined.

Fatigue Tests

Since the composite femur was made from short E-glass fibers/epoxy resin and solid rigid polyurethane foam, its deformation behavior and strength could be affected by cyclic loading. Therefore, the fatigue test of LCPs was carried out using a 4-point bending specimen (Figure 3), that is, an LCP fixed on two cylinders (polyvinyl chloride pipe reinforced with epoxy resin). Since the deformation of LCP is limited with the closure of fracture gap, the stress-controlled fatigue test using a 4-point bending specimen may not represent the actual situation. In the present work, the actual strains on LCP (taking into account of the closure of fracture gap, bone geometry, and bone properties) were first obtained from the monotonic loading model (previous section), and then used in the strain-controlled fatigue tests. During fatigue tests, the strains distributed on the surface of LCP were controlled to match with those of the monotonic loading model by

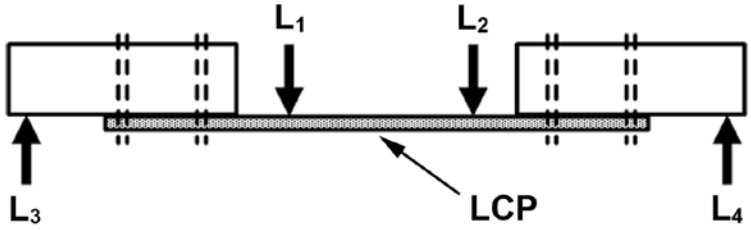

Figure 3 — Experimental system for cyclic loading of 4-point bending specimen.

adjusting the load positions (L_1 to L_4) as well as the displacements of 4-point bending device (Figure 3). Thus, the influences of fracture-gap closure, bone geometry, and bone properties on deformation of LCP could be taken into account during fatigue test.

The strain-controlled fatigue tests (sinusoidal waveform with 3-Hz frequency and 0.1 strain ratio) were performed by using a servo-hydraulic fatigue machine (Instron 8872 with 5-kN load cell) under 25°C and 55% relative humidity. The fatigue failure was defined as a complete fracture of LCP. For the present work, it was assumed that one load cycle per leg took 2 s, the patient walked 30 min a day, and the adequate healing of fracture to sustain full load of walking without walking aid occurred within 6 months. Once the femur was fully healed, the LCP was no longer under severe loading. Based on this assumption, an LCP would be cyclically loaded about 165,000 cycles before healing. To ensure the durability of LCP, the fatigue tests were performed beyond the 165,000 cycles and stopped in the situation that no fatigue failure occurred after 1,000,000 cycles of loading. During fatigue tests, the applied load, displacement of a 4-point bending device, strain distribution on the surface of LCP, and time were simultaneously recorded 100 times in each cycle with computer-controlled data acquisition. After fatigue tests, the screw torque was checked for of screw loosening. The fatigue tests of each model were repeated three times (n = 3) using new LCPs. The means and SDs of fatigue life were calculated. The CIs with significant level (α) of 0.05 were also determined.

Results

Stiffness and Strain Distribution

The 1-mm fracture gaps of models 2 and 3 were closed immediately after compression load of 5 N, whereas the 8-mm fracture gaps of models 4 and 5 were closed after compression load of 400 N. None of screw loosening or plastic deformation occurred for each model after loading. As a ratio between compression load and deformation of femoral model, the stiffnesses of all models were determined, as follows.

Model 1: The stiffness of intact femur was 284 N/mm (3.96 SD and 3.47 CI).

Model 2: The stiffness after contact of medial cortexes on fracture gap was 270 N/mm (2.59 SD and 2.27 CI).

Model 3: The stiffness after contact of medial cortexes on fracture gap was 285 N/mm (3.54 SD and 3.10 CI).

Model 4: The stiffness before the contact of medial cortexes on fracture gap was 27 N/mm (1.30 SD and 1.14 CI), whereas those after the contact of medial cortexes on fracture gap were 155 N/mm (3.54 SD and 3.10 CI).

Model 5: The stiffness before the contact of medial cortexes on fracture gap was 24 N/mm (1.79 SD and 1.57 CI), whereas those after the contact of medial cortexes on fracture gap were 170 N/mm (3.49 SD and 3.06 CI).

The strain distributions on the LCP surfaces of femoral models with 1-mm fracture gap and those with 8-mm fracture gap are shown in Figure 4. For 1-mm fracture gaps, the maximum tensile strain of the long column fixation model (model 2) was 73 με (1.92 SD and 1.68 CI), while the maximum tensile strain of 88 με (3.16 SD and 2.77 CI) was observed for short column fixation model (model 3). On the other hand, the maximum tensile strain on the LCP surface of 8-mm fracture gap models were 2,210 με (6.14 SD and 5.38 CI) and 2,365 με (9.84 SD and 8.62 CI) for long column fixation model (model 4) and short column fixation model (model 5), respectively.

Fatigue Life

After 1,000,000 cycles of loading, there was no fracture of LCP occurred on 1-mm fracture gap models (models 2 and 3). On the other hand, the complete fractures of LCPs occurred after 51,500 cycles (2,021 SD and 2,287 CI) and 42,000 cycles (3,512 SD and 3,974 CI) for model 4 and 5 (8-mm fracture gap models), respectively. After fatigue tests, the screw torques were checked and no screw loosening was detected. Similar fatigue crack initiation and propagation were observed for model 4 and 5, i.e., fatigue cracks occurred at the middle of LCP (Figure 5). The present locations of fatigue cracks corresponded to the location of maximum stress calculated from finite element method (Frigg, 2003; Stoffel et al., 2003). The mechanisms of crack initiation and propagation of LCP have been discussed in detail elsewhere (Kanchanomai et al., 2008).

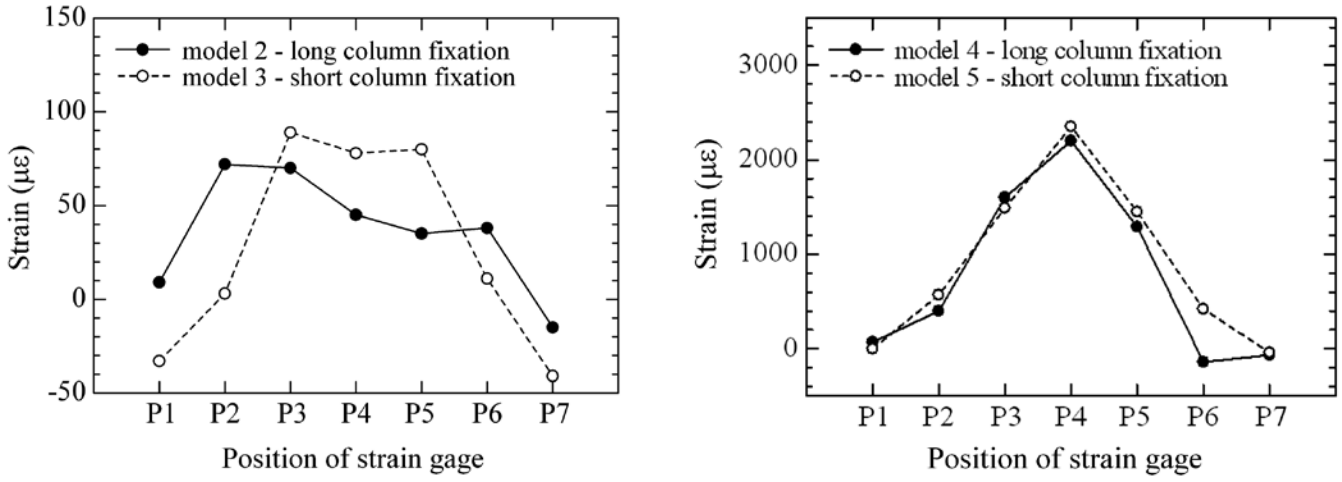

Figure 4 — Strain distributions on the LCP surfaces of (*left*) femoral models with 1-mm fracture gap size (models 2 and 3), and (*right*) femoral models with 8-mm fracture gap size (models 4 and 5).

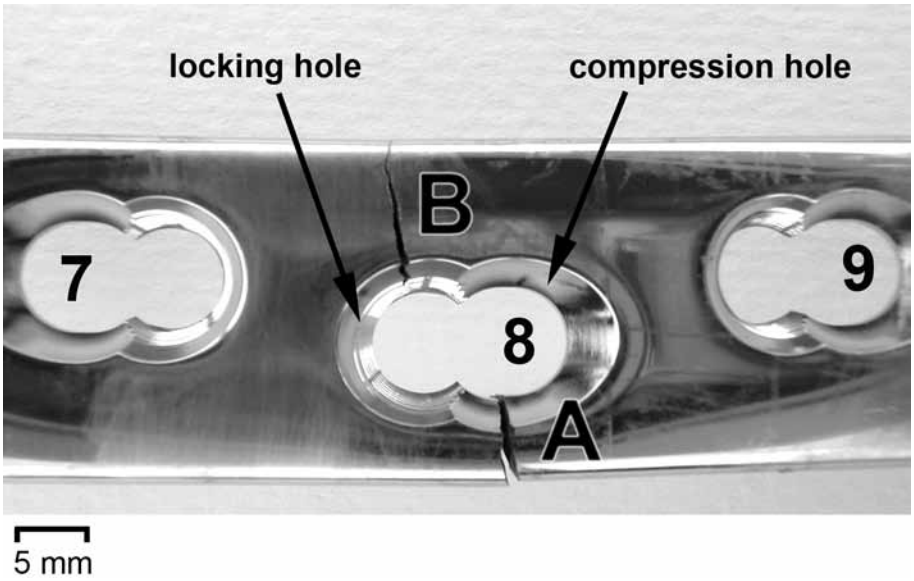

Figure 5 — Fatigue cracks at the middle of LCP (crack A on compression hole, and crack B on locking hole).

Discussion

In 1-mm fracture gap models (models 2 and 3), the large contact areas of fracture surfaces resulted in nearly similar stiffness to that of intact femur (model 1), i.e., the 270–290 N/mm range. In other words, the plated area of femur could be protected, and the stiffness was maintained by LCP. In contrast, smaller contact areas of fracture surfaces were observed for 8-mm fracture gap models (models 4 and 5). The stiffnesses of models 4 and 5 were in the range of 155–170 N/mm, which could not maintain the stiffness similar to that of the intact femur (model 1). For 8-mm transverse fracture (comminuted fracture) at the middle of diaphysis fixed with an LCP, the full load of weight bearing should be avoided in early phase of treatment.

For similar applied load and fracture gap size, the energies absorbed by long column fixation models and short column fixation models were similar. This energy resulted in the deformation of LCP, especially in the fracture area of femur. Since there was more volume of LCP for long column fixation models (models 2 and 4) than that of short column fixation models (3 and 5), the absorbed energy per unit volume of short column fixa-

tion models was higher than that of long column fixation models. The higher absorbed energy per unit volume of short column fixation models resulted in higher strains on the surfaces of LCPs than those of long column fixation models (Figure 4).

As a process of cumulative damage with increasing number of cycles, the fatigue life is shorter for material under higher cyclic stress. The relationship between cyclic stress and fatigue life follows a power law; that is, a small amount of reduction in cyclic stress results in a significant improvement of fatigue life. However, there is a distinct stress level (fatigue limit or endurance limit) below which the fatigue life becomes very long (Suresh, 1998). Since 1-mm fracture gap models (models 2 and 3) were cyclically loaded until 1,000,000 cycles without any fatigue failure, it is likely that the tensile stresses on LCPs of these models were lower than the fatigue limit of 316L stainless steel. Moreover, the actual load supported by LCP was not constant but decreased as the bone healing progressed. Therefore, the possibility of fatigue failure of LCP was no longer critical for models 2 and 3. For the above reasons, earlier partial weight bearing after plating could be allowed in the patient with 1-mm or less transverse fracture at the middle of diaphysis.

In contrast, the tensile strains on LCPs of 8-mm fracture gap models (models 4 and 5) were significantly higher than those of 1-mm fracture gap models (2 and 3). It is likely that the tensile stresses on LCPs of 8-mm fracture gap models were higher than the fatigue limit of 316L stainless steel. The complete fractures of LCPs occurred after 51,500 and 42,000 cycles of loading for model 4 (long column fixation on 8-mm fracture gap) and for model 5 (short column fixation on 8-mm fracture gap), respectively. For the present work, it was assumed that one load cycle per leg took 2 s, the patient walked 30 min a day, and the adequate healing of fracture to sustain the full load of walking without walking aid occurred within 6 months. Based on this assumption, the complete fracture of LCP of model 4 at 51,500 cycles of loading and that of model 5 at 42,000 cycles of loading were equivalent to about 57 and 47 days of walking, respectively. Therefore, the fatigue failure of LCP was possible before the adequate healing of fracture; and the full load of walking should be avoided for the patient treated with plating on a significant medial gap condition or comminuted fracture.

To emphasize the clinical relevance of the present findings, a case of fatigue failure of LCP fixed on comminuted fracture of femur was studied. A 47 year-old male had fractures of right femur and right clavicle. After débridement, the fracture was fixed with 16-hole stainless steel broad LCP. The patient was instructed to bear partial weight after treatment. Unfortunately, the broken plate and hypertrophic nonunion of facture site were observed after 6 months of treatment as shown in Figure 6. Similar to the present biomechanical study (Figure 5), fatigue cracks were seen at both compression hole and locking hole located at the middle of LCP. The way of fixation, partial loading, and the load bearing from callus as well as muscle may result in longer fatigue life of LCP than that of present biomechanical study.

Figure 6 — Fatigue failure of LCP fixed on a fractured femur of 47-year-old male after 6 months of bearing partial weight.

There are some other factors that may affect the fatigue life of the plate, such as the location of fracture, type and complexity of fracture, load acting on the plate, stance speed, bone elasticity, and types and sizes of plate. The effects of these factors on the fatigue life of the plate are complicated but crucial in clinical uses. Unfortunately, the present biomechanical study has been done under controlled conditions. Therefore, more considerations should be added to the present findings during clinical practice.

Acknowledgments

The authors would like to acknowledge the discussions and support from S. Rodkwan (Kasetsart University, Thailand), the Thailand Research Fund, the National Research Council of Thailand, the Commission on Higher Education of Thailand, and the National Metal and Materials Technology Center.

References

Aslam, N., Hazarika, S., Nagarajah, K., & McNab, I. (2005). AO 2 mm locking compression plate for arthrodesis of the proximal interphalangeal joint. *Injury Extra, 36,* 428–431.

Azevedo, C.R.F. (2003). Failure analysis of a commercially pure titanium plate for osteosynthesis. *Engineering Failure Analysis, 10,* 153–164.

Cordey, J., Borgeaud, M., Frankle, M., Harder, Y., & Martinet, O. (1999). Loading model for the human femur taking the tension band effect of the ilio-tibial tract into account. *Injury, 30,* SA26–SA30.

Cristofolini, L., Cappello, A., Viceconti, M., & Toni, A. (1996). Mechanical validation of whole bone composite femur models. *Journal of Biomechanics, 29,* 525–535.

Frigg, R. (2003). Development of the Locking Compression Plate. *Injury, 34,* 6–10.

Heiner, A.D., & Brown, T.D. (2001). Structural properties of a new design of composite replicate femurs and tibias. *Journal of Biomechanics, 34,* 773–781.

Kanchanomai, C., Phiphobmongkol, V., & Muanjan, P. (2008). Fatigue failure of an orthopedic implant – A locking compression plate. *Engineering Failure Analysis, 15,* 521–530.

Leung, F., Zhu, L., Ho, H., Lu, W.W., & Chow, S.P. (2003). Palmar plate fixation of AO type C2 fracture of distal radius using a locking compression plate - A biomechanical study in a cadaveric model. *The Journal of Hand Surgery, 28,* 263–266.

Sivakumar, M., Kamachi Mudali, U., & Rajeswari, S. (1994). Investigation of failures in stainless steel orthopaedic implant devices: fatigue failure due to improper fixation of a compression bone plate. *Journal of Materials Science Letters, 13,* 142–145.

Sommer, C., Gautier, E., Muller, M., Helfet, D.L., & Wagner, M. (2003). First clinical results of the locking compression plate (LCP). *Injury, 34,* 43–54.

Stoffel, K., Dieter, U., Stachowiak, G., Gachter, A., & Kuster, M.S. (2003). Biomechanical testing of the LCP - how can stability in locked internal fixators be controlled? *Injury, 34,* 11–19.

Sudhakar, K.V. (2005). Investigation of failure mechanism in vitallium 2000 implant. *Engineering Failure Analysis, 12,* 257–262.

Suresh, S. (1998). *Fatigue of materials*. New York: Cambridge University Press.

Thakur, A.J. (1997). *The elements of fracture fixation*. Glasgow Churchill Livingstone.

Van Meeteren, M.C., Van Riet, Y.E.A., Van Der Werken, C.H.R., & Roukema, J.A. (1996). Condylar plate fixation of subtrochanteric femoral fractures. *Injury, 27,* 715–717.

Waide, V., Cristofolini, L., Stolk, J., Verdonschot, N., & Toni, A. (2003). Experimental investigation of bone remodelling using composite femurs. *Clinical Biomechanics (Bristol, Avon), 18,* 523–536.